



## Structural and Optical Properties for Zn Doped CdO Thin Films Prepared by Pulse Laser deposition

Dhia Aldin Sleibi Mustafa<sup>\*1</sup>, Rawaa Isam Mohammed Al-Rawi<sup>2</sup>

<sup>1</sup>Iraqi Sunni Affairs, Baghdad, Iraq.

<sup>2</sup> Department of Physics, College of Education for pure Sciences, Al-Anbar University, Al-Anbar, Iraq.

### Abstract

In this work, the effect of Zn dopant on structural and optical properties of cadmium oxides, CdO, thin film were studied prepared by pulse laser deposition on glass substrate then annealed at 250 °C in air. All films were examined by X-ray diffraction and UV- visible spectrometer. The XRD analysis shows appearance of new phase identical with hexagonal ZnO additional with cubic phase at high Zn content, which effected on the optical properties. The optical energy gap increase from 2.45 eV to 2.70 eV with increasing Zn content from 0 to 40 %.

**Keywords:** Zn doped CdO, pulse laser, structural, optical properties.

### الخواص التركيبية والضوئية للأغشية الرقيقة للزنك المطعم بأوكسيد الكاديوم المحضر بواسطة الترسيب النبضي لليزر

ضياء الدين صليبي مصطفى<sup>\*1</sup>، رواء عصام محمد الراوي<sup>2</sup>

<sup>1</sup>ديوان الوقف السني، دائرة المؤسسات الإسلامية والخيرية، أوقاف الكرخ، بغداد، العراق.

<sup>2</sup>قسم الفيزياء، كلية التربية للعلوم الصرفة،<sup>2</sup> جامعة الأنبار.

### الخلاصة

في هذا العمل جرت دراسة تأثير الزنك المطعم على الخصائص التركيبية والبصرية لأغشية أوكسيد الكاديوم، والتي تم تحضيرها بواسطة الترسيب النبضي لليزر الرقيقة على شريحة من الزجاج بعد تقسيته عند 250 درجة مئوية في الهواء. جميع الأغشية الرقيقة تم فحصها بواسطة حيود الأشعة السينية والمطياف فوق البنفسجي-المرئي. وقد بينت تحليلات حيود الأشعة السينية وجود طور جديد يماثل أوكسيد الزنك ZnO بالإضافة إلى الطور المكعبي عند تراكيز عالية للزمن، والذي أثر على الخصائص البصرية. بينت النتائج زيادة فجوة الطاقة البصرية من 2.45 eV إلى 2.70 eV مع زيادة تركيز الزنك من 0 إلى 40%.

### Introduction

CdO is an important n-type semiconductor with a cubic structure, which belongs to the II–VI with a direct band gap of 2.5 eV , having a simple cubic structure [1].

Synthesis techniques and conditions can considerably affect the properties of CdO films[1].CdO films prepared by different ways such as chemical bath deposition[2],spray pyrolysis [3], pulsed laser deposition [4]andsol- gel [5].

Low electrical resistivity and high transmission in the visible region [6] make it possible to use in various fields with many applications such as solar cells, phototransistors,transparent electrodes, gas

\*Email: diaa\_10\_71@yahoo.com

sensors [7] and used as antibacterial [8-9], aim of my work effect of zinc doped cadmium oxide on the structural and optical properties for thin films prepared

### Experimental part

Prior to deposition, the substrates were cleaned with cleaner solution, distilled water and followed by alcohol using ultrasonic bath. Films thicknesses were determined using Michelson interferometer. Pure and Zn doped cadmium oxide pellet were prepared by mix (0, 10, 15, 20, 30 and 40) % Zn: CdO atom ratio by mechanical mortar with steel balls for 10 minutes. A piston under a pressure of 2.5 tons was used to make a pellet of 1.4 cm diameter shown in Figure-1. The targets were bombarded by Nd:YAG pulse laser (HuaFei Tong Da Technology –Diamond -288 Pattern EPLS) at 6 Hz frequency and 9 ns pulse duration with 1064 nm wavelength with 800 mJ to produce thin films onto glass substrates attached about 2 cm above the target in glass chamber under vacuum of  $1 \times 10^{-3}$  mbar achieved using double stage rotary. The prepared films then annealed at 250°C temperature.

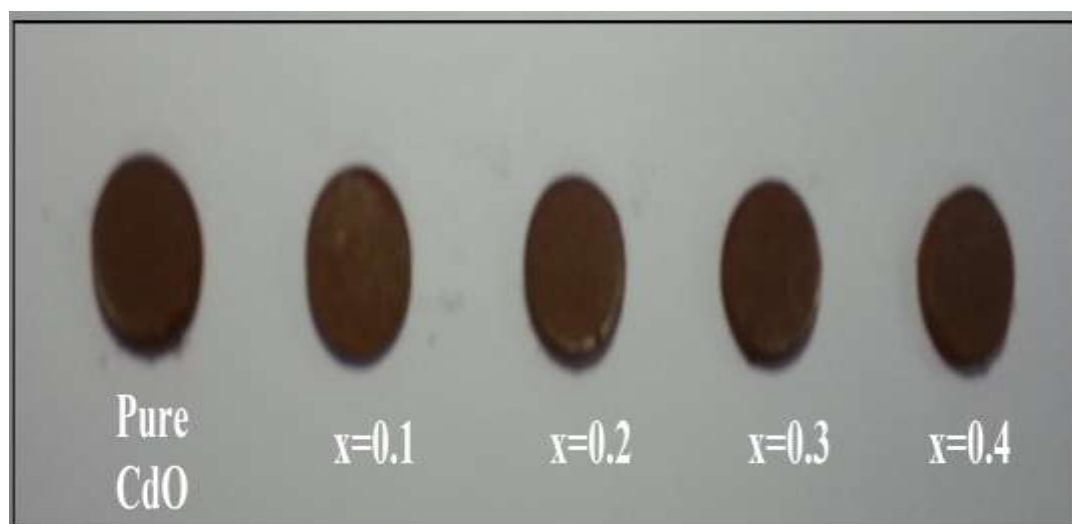


Figure 1-(CdO)<sub>1-x</sub>Zn<sub>x</sub> pellets with different Zn ratio.

X-ray diffraction (XRD) pattern of the deposited films on Corning glass substrate were examined by SHIMADZU XRD-6000 X-ray diffractometer in  $2\theta$  range from 20° to 80°.

The inter-planer distances  $d_{hkl}$  are measured using Bragg law [10]

$$2 d_{hkl} \sin \theta = m \lambda \quad (1)$$

Where  $\theta$  is the diffraction angle,  $m$  is the diffraction order,  $\lambda$  is the X-ray wavelength for Cu-K $\alpha$  transition which equal to 1.5406 Å

The average crystallite size was determined by Scherrer's formula [11]:

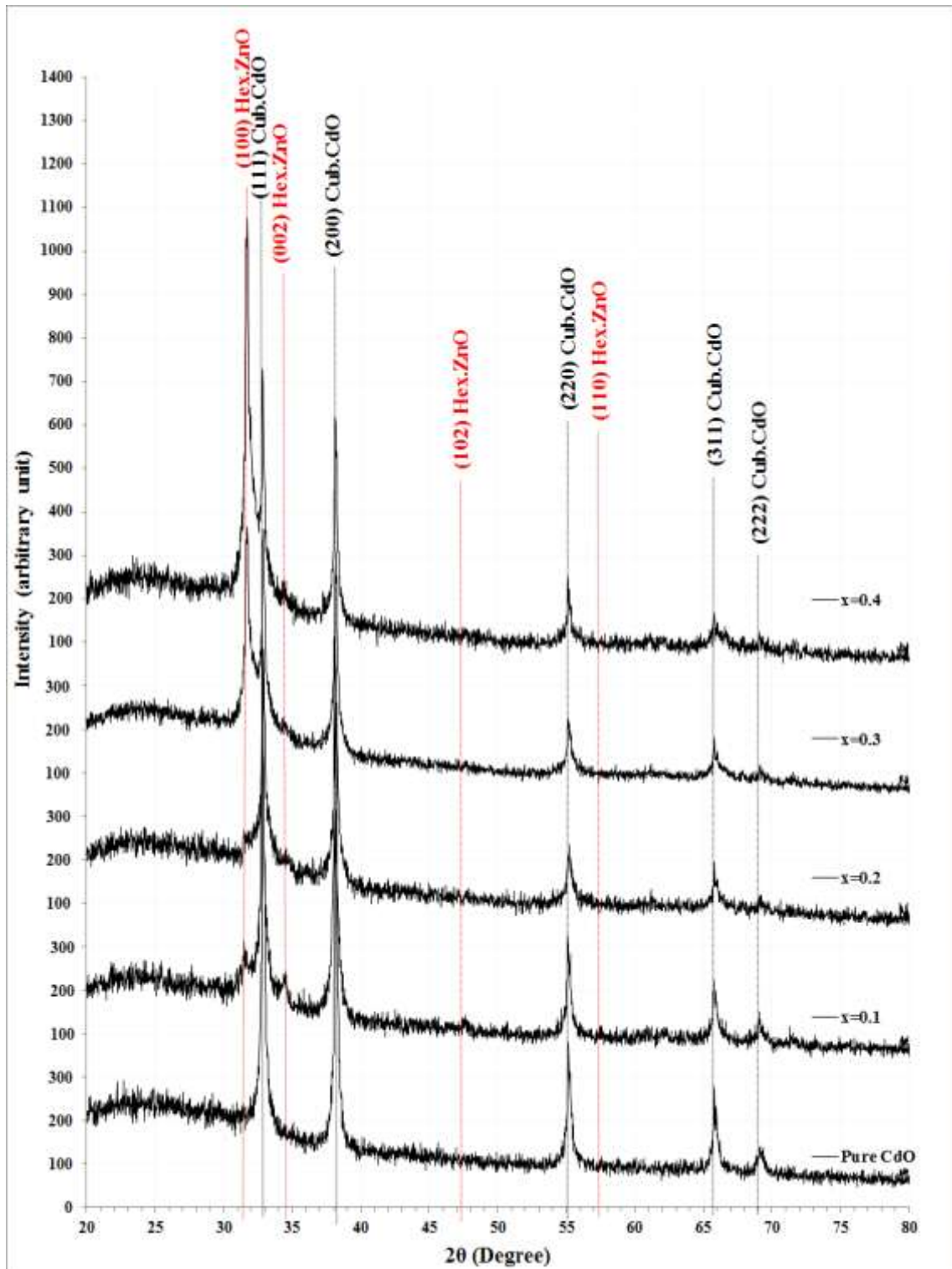
$$C.S = \frac{0.89 \lambda}{\Delta(2\theta) \cdot \cos(\theta)} \quad (2)$$

Optical transmittance spectrum were recorded, at room temperature, in the wavelength range 300-1100 nm using OPTIMA SP-3000 UV-VIS spectrophotometer.

### Results and discussion

Figure-2 Shows XRD for pure and Zn doped CdO thin film deposited on glass, it shows a polycrystalline structure for all films where five peaks located in CdO sample at  $2\theta = 32.8631, 38.1425, 55.1536, 65.7961$  and  $69.1480^\circ$  corresponding to (111), (200), (220), (311) and (222) respectively identically with standard inter-planer distance values ( $d_{hkl}$ ). another phase appears for hexagonal ZnO at high Zn content with preferred orientation along (100) direction at  $2\theta = 31.7318^\circ$

It is clear that increasing Zn content cause to improve the (CdO)<sub>1-x</sub>Zn<sub>x</sub> thin films crystallinity.



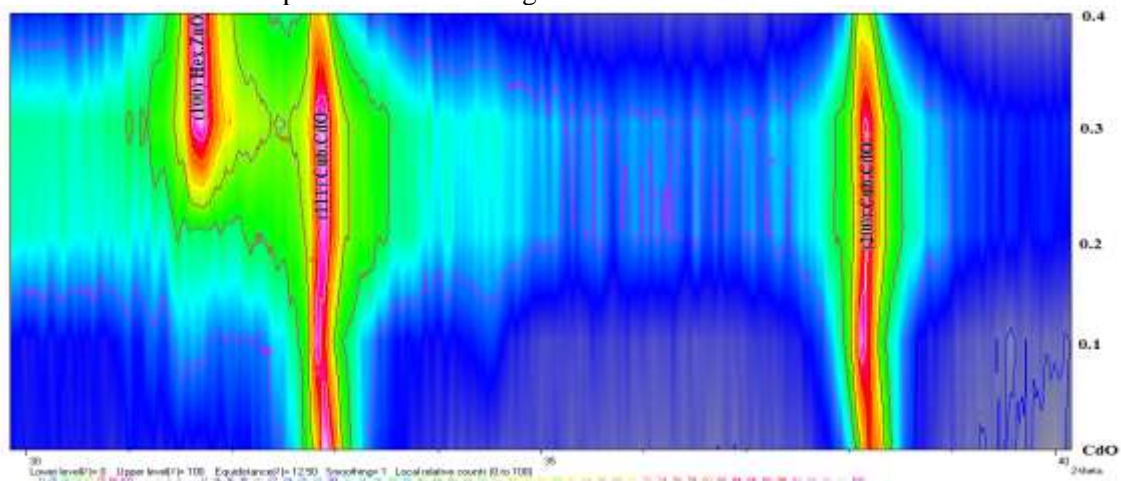
**Figure 2**-X-ray diffraction patterns for  $(\text{CdO})_{1-x}\text{Zn}_x$  thin films deposited by pulse laser energy with different ratio annealed at  $250^\circ\text{C}$ .

Table-1 shows the experimental peak location and their inter-planer distance  $d_{hkl}$  compared with standard  $d_{hkl}$  from International center for diffraction data card No. 96-900-8610. Also contain the full width at half maximum FWHM and crystalline size (C.S), calculated by Scherrer formula, for pure and doped cadmium oxides films. This table shows that increasing zinc content leads to increase the average crystalline size.

**Table 1**-Structural parameters for  $(\text{CdO})_{1-x}\text{Zn}_x$  thin films deposited by pulse laser energy with different ratio annealed at  $250^\circ\text{C}$ .

x	2 $\theta$ (Deg.)	FWHM (Deg.)	$d_{hkl}$ Exp.( $\text{\AA}$ )	C.S (nm)	$d_{hkl}$ Std.( $\text{\AA}$ )	Phase	hkl	card No.
0	32.8631	0.3771	2.7232	22.0	2.7108	Cub. CdO	(111)	96-900-8610
	38.1425	0.3352	2.3575	25.1	2.3477	Cub. CdO	(200)	96-900-8610
	55.1536	0.3771	1.6639	23.8	1.6600	Cub. CdO	(220)	96-900-8610
	65.7961	0.4609	1.4182	20.5	1.4157	Cub. CdO	(311)	96-900-8610
	69.1480	0.5028	1.3574	19.2	1.3554	Cub. CdO	(222)	96-900-8610
0.1	31.4385	0.5028	2.8432	16.4	2.8137	Hex. ZnO	(100)	96-901-1663
	32.9050	0.2514	2.7198	32.9	2.7108	Cub. CdO	(111)	96-900-8610
	38.1425	0.3771	2.3575	22.3	2.3477	Cub. CdO	(200)	96-900-8610
	47.6117	0.5447	1.9084	15.9	2.6035	Hex. ZnO	(002)	96-901-1663
	55.1117	0.4609	1.6651	19.4	1.6600	Cub. CdO	(220)	96-900-8610
	65.7961	0.4609	1.4182	20.5	1.4157	Cub. CdO	(311)	96-900-8610
0.2	31.4385	0.5866	2.8432	14.1	2.8137	Hex. ZnO	(100)	96-901-1663
	32.7793	0.2514	2.7299	32.9	2.7108	Cub. CdO	(111)	96-900-8610
	38.1006	0.2933	2.3600	28.7	2.3477	Cub. CdO	(200)	96-900-8610
	55.2374	0.4609	1.6616	19.5	1.6600	Cub. CdO	(220)	96-900-8610
	65.7961	0.5028	1.4182	18.8	1.4157	Cub. CdO	(311)	96-900-8610
	69.1480	0.6704	1.3574	14.4	1.3554	Cub. CdO	(222)	96-900-8610
0.3	31.7318	0.3352	2.8176	24.6	2.8137	Hex. ZnO	(100)	96-901-1663
	32.9050	0.2095	2.7198	39.5	2.7108	Cub. CdO	(111)	96-900-8610
	38.1844	0.2514	2.3550	33.4	2.3477	Cub. CdO	(200)	96-900-8610
	55.1536	0.3771	1.6639	23.8	1.6600	Cub. CdO	(220)	96-900-8610
	65.7542	0.3771	1.4190	25.1	1.4157	Cub. CdO	(311)	96-900-8610
	69.1061	0.3352	1.3581	28.8	1.3554	Cub. CdO	(222)	96-900-8610
0.4	31.7318	0.3352	2.8176	24.6	2.8137	Hex. ZnO	(100)	96-901-1663
	32.8212	0.2095	2.7265	39.5	2.7108	Cub. CdO	(111)	96-900-8610
	38.1425	0.2514	2.3575	33.4	2.3477	Cub. CdO	(200)	96-900-8610
	55.1117	0.3352	1.6651	26.7	1.6600	Cub. CdO	(220)	96-900-8610
	65.7961	0.3771	1.4182	25.1	1.4157	Cub. CdO	(311)	96-900-8610
	69.0642	0.4609	1.3589	20.9	1.3554	Cub. CdO	(222)	96-900-8610

Figure-3 Shows two dimensional view for (111) and (200) peaks for CdO and (100) peak for ZnO appear in  $(\text{CdO})_{1-x}\text{Zn}_x$  films. It shows appearance of the new phase (Hex. ZnO) at 25% Zn content, and decrease the Cub. CdO phase with increasing Zn ratio.

**Figure 3**-2D view for (111) and (200) peaks for CdO and (100) peak for ZnO for different Zn ratio.

Optical properties of  $(\text{CdO})_{1-x}\text{Zn}_x$  films deposited on glass substrate were done in the wavelength range 300–1100 nm. Figure -4 shows the transmission spectra for prepared samples at different Zn content. This figure shows a blue shift in spectra with increasing dopant ratio.

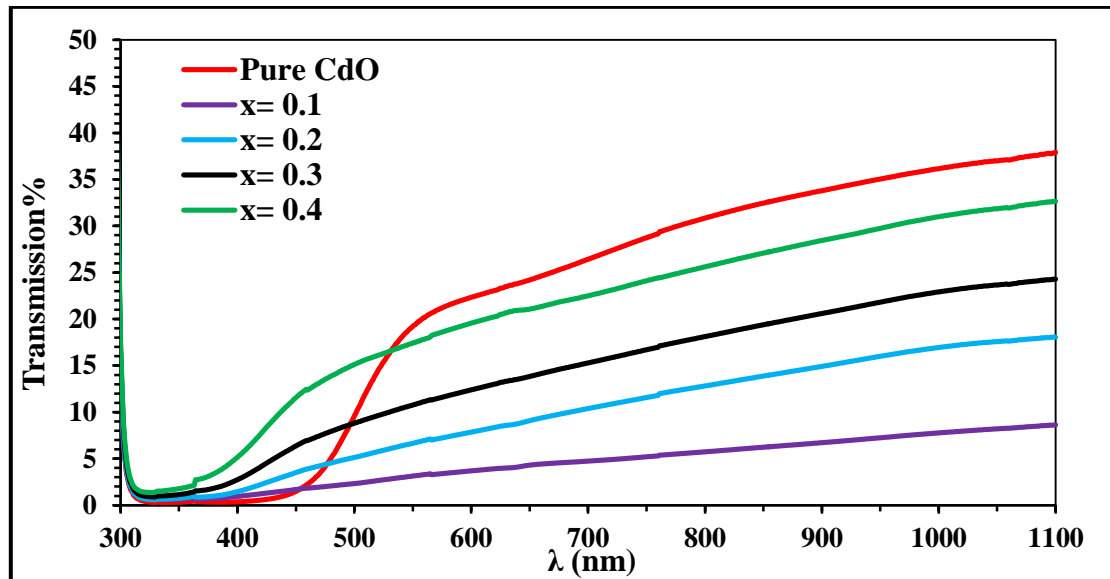


**Figure 4-**Transmission spectrum for  $(\text{CdO})_{1-x}\text{Zn}_x$  thin films deposited by pulse laser with different ratio annealed at 250°C.

To calculate optical energy gap values ( $E_g^{\text{opt}}$ ) for  $(\text{CdO})_{1-x}\text{Zn}_x$  thin films were determined using Tauc equation by plotting the relation between  $(\alpha h\nu)^2$  versus photon energy ( $h\nu$ ), it is found that the allowed direct transition calculated from the portion at  $(\alpha h\nu)^2 = 0$  as shown in Figure-5. It is clear from this figure that the energy gap increases with increasing zinc content.

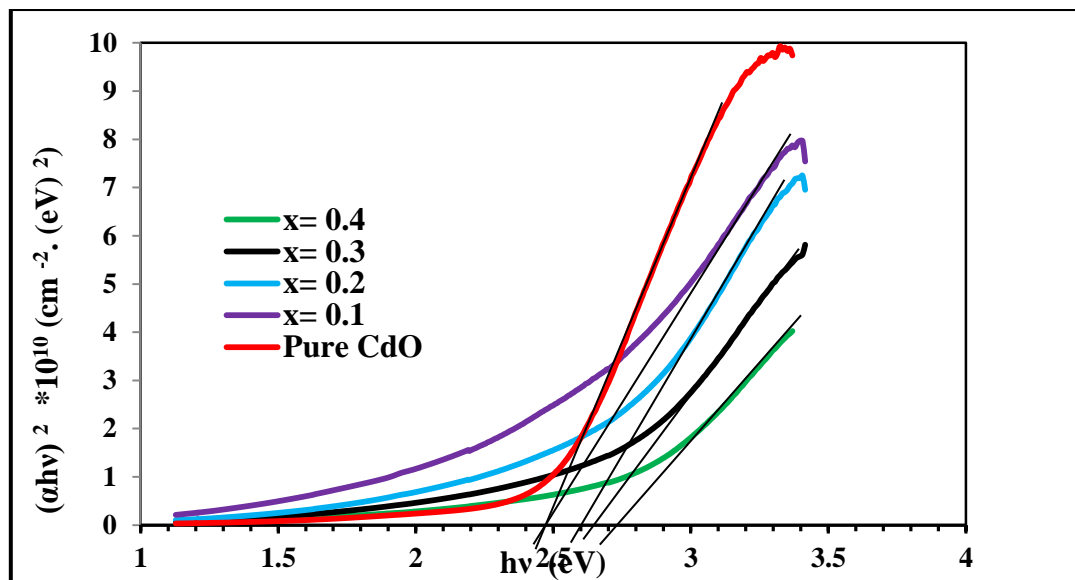


**Figure 5-**Variation of  $(\alpha h\nu)^2$  versus photon energy ( $h\nu$ ) for  $(\text{CdO})_{1-x}\text{Zn}_x$  thin films deposited by pulse laser with different ratio annealed at 250°C

The relation between the extinction coefficient and wavelength for  $(\text{CdO})_{1-x}\text{Zn}_x$  films deposited at different annealing temperatures is shown in Figure-6. From this figure we can see that the extinction coefficient ( $k$ ) takes the similar behavior of the corresponding absorption coefficient.

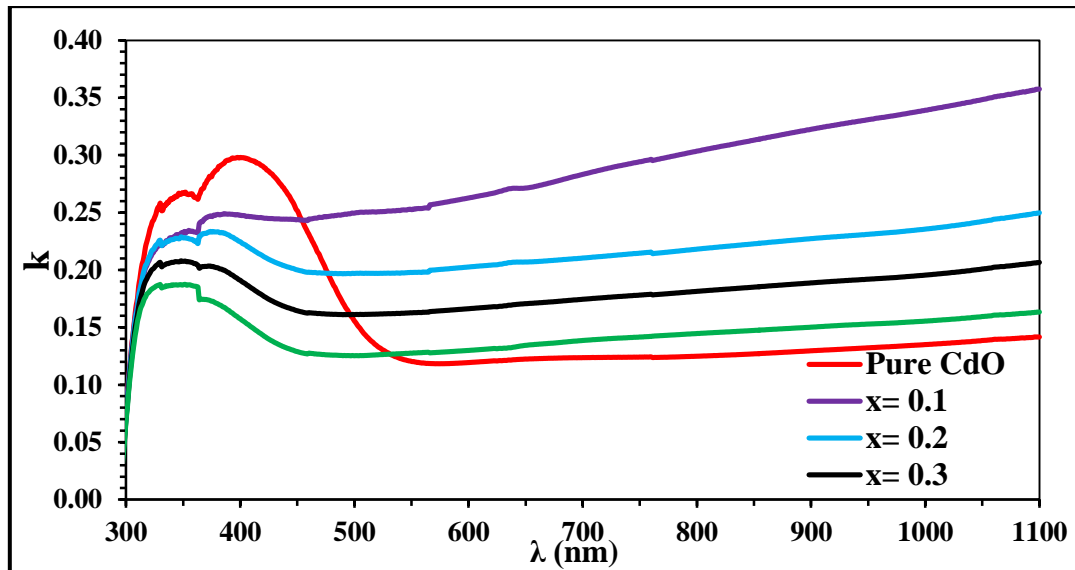


**Figure 6**-Extinction coefficient ( $k$ ) with the wavelength for  $(\text{CdO})_{1-x}\text{Zn}_x$  thin films deposited by pulse laser with different ratio annealed at  $250^\circ\text{C}$ .

Real and imaginary part of dielectric constant were determined using equations. The plot of real and imaginary ( $\epsilon_r, \epsilon_i$ ) parts of the Dielectric constant with wavelength for  $(\text{CdO})_{1-x}\text{Zn}_x$  thin deposited for annealing temperature ( $250$ ) C as shown in Figures- (7, 8), respectively. It depends mainly on the extinction coefficient values according to the relationship between them.

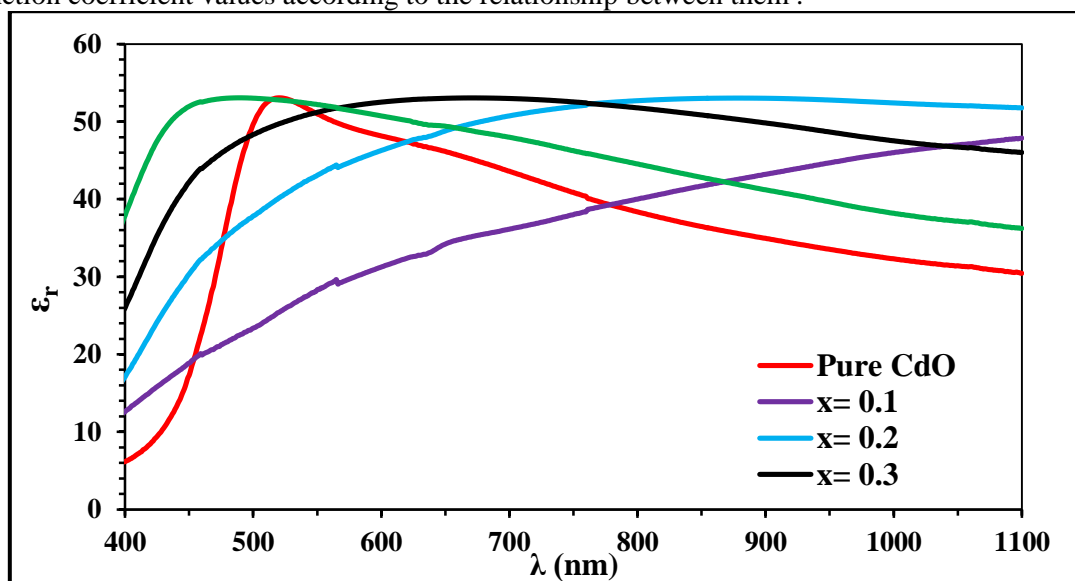


**Figure 7**-Real part of dielectric constant with the wavelength for  $(\text{CdO})_{1-x}\text{Zn}_x$  thin films deposited by pulse laser with different ratio annealed at  $250^\circ\text{C}$ .

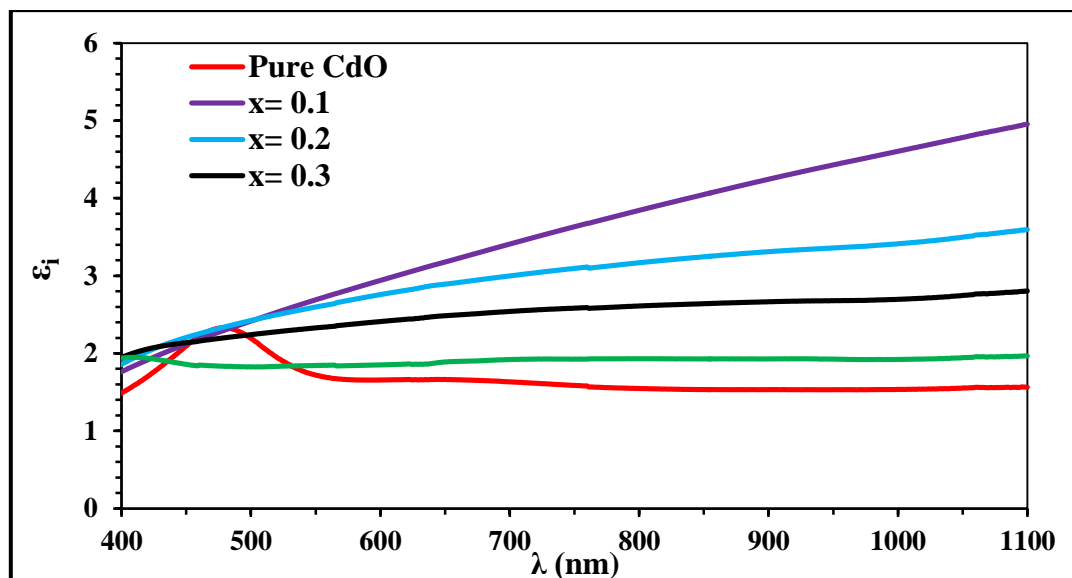


**Figure 8-**Imaginary part of dielectric constant with the wavelength for  $(\text{CdO})_{1-x}\text{Zn}_x$  thin films deposited by pulse laser with different ratio annealed at  $250^\circ\text{C}$ .

Figure-9 shows the variation in refractive index with wavelength for  $(\text{CdO})_{1-x}\text{Zn}_x$  thin films in the wavelength range of (300-1100)nm for annealing temperature ( $250^\circ\text{C}$ ) and . It is observed that the refractive index, in general, increases slightly with increases of concentration .The refractive index of perovskite thin film is known to be proportional to the distance between atomic planes .This result can be explained by an increase in the density of the film due to better packing and increased crystallinity

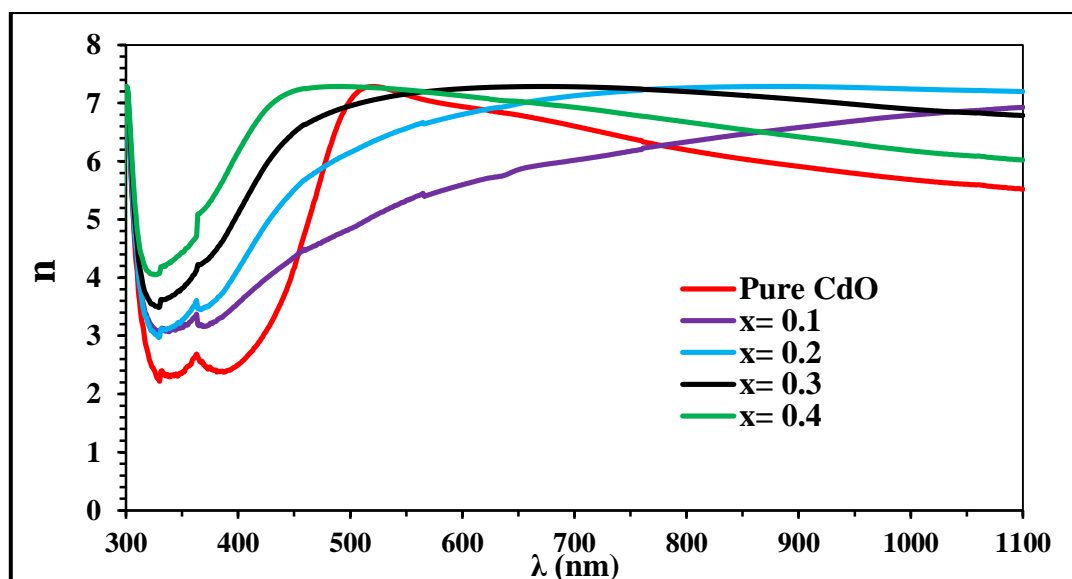


**Figure 9-**Refractive index with the wavelength for  $(\text{CdO})_{1-x}\text{Zn}_x$  thin films deposited by pulse laser with different ratio annealed at  $250^\circ\text{C}$ .

Table-2 shows the calculated optical constants at 500 nm wavelength and energy gap for  $(\text{CdO})_{1-x}\text{Zn}_x$  thin films, deposited by pulse laser with 800 mJ pulses energy using 500 pulses, with different Zn contents. The pure CdO film shows a band gap of 2.45 eV, while increasing Zn content to 0.4 leads to an increase in the energy gap to 2.7 eV. This increment may be due to the existence of another phase with a hexagonal structure with increasing (x). The highest transmission values are at  $x=0.4$ .

**Table 2-**Optical constants at 500 nm wavelength and (Eg) values length for (CdO)<sub>1-x</sub>Zn<sub>x</sub> thin films deposited by pulse laser with different ratio of Zn

x	T%	$\alpha$ (cm <sup>-1</sup> )	K	n	$\epsilon_r$	$\epsilon_i$	Eg (eV)
0	9.59	39078	0.156	7.048	49.655	2.193	2.45
0.1	2.33	62680	0.250	4.841	23.370	2.416	2.45
0.2	5.14	49468	0.197	6.153	37.827	2.424	2.60
0.3	8.82	40471	0.161	6.954	48.336	2.241	2.65
0.4	15.13	31474	0.125	7.282	53.019	1.825	2.70

### Conclusions

Structural and optical properties (CdO)<sub>1-x</sub>Zn<sub>x</sub> thin films deposited by pulse laser deposition technique with different ratio have been studied at different Zn content. A polycrystalline structure for all films and identical with standard card for cubic CdO crystal at low Zn content then another phase appears for Hexagonal ZnO at high Zn content, with enhancement the crystalline and increasing the average crystalline size. The transmittance increases with increasing with increasing Zn content. Also, the energy gap increases from 2.45 eV to 2.70 eV with the increase of Zn content from 0 to 40 %

### References

1. Yufanyi, D.M., Tendo, J.F., Ondoh, A.M. and Mbadcam, J.K. **2014**. CdO Nanoparticles by Thermal Decomposition of a Cadmium- Hexamethylenetetramine Complex. *J. Mater. Sci. Res.*, **3**(3): 1–11.
2. Ocampo, M., Sebastian, P.J. and Campos, J. **1994**. Chemically deposited n-CdO thin films for solar cell applications. *Phys. Stat. Sol. A* **143** K29.
3. Gurumurugan, K., Mangalaraj, D., Narayandass, Sa. K., Sekar K., Girija Vallabhan C.P. **1994**. Characterization of transparent conducting CdO films deposited by spray pyrolysis. *Semicond. Sci. Tech.* **9**(10).
4. Yan M., Lane M., Kannewurf C. R. and Chang R.P.H. **2001**. Highly conductive epitaxial Cdo thin films prepared by pulsed laser depositio. *Appl. Phys. Lett.* **78**, 133.
5. Ilican, S., Caglar, M., Caglar, Y. and Yakuphanoglu, F. **2009**. CdO:Al films deposited by sol-gel process: A study on their structural and optical properties. *Optoelectron. Adv. Mater. Rapid Commun.*, **3**(2): 135–140.
6. Tabatabaee, M., Mozafari, A.A., Ghassemzadeh, M., Nateghi, M.R. and Abedini, I. **2013**. A Simple Method for Synthesis of Cadmium Oxide Nanoparticles Using Polyethylene Glycol. *Bulg. Chem. Commun.* **45**(1): 90–92.
7. Kondawar, S. **2011**. Electrical Conductivity of Cadmium Oxide Nanoparticles Embedded Polyaniline Nanocomposites. *Adv. Appl. Sci. Res.*, **2**(4): 401–406.
8. Al Marjani, M.F. and Kadham, Z.A. **2016**. Antibacterial Activity Of Cadmium Oxide Nanoparticles Synthesized By Chemical Method. *J. Multidiscip. Eng. Sci. Technol.*, **3**(6): 5007–5011.
9. Sakthivel, S. and Mangalaraj, D. **2011**. Cadmium Oxide Nano Particles by Sol-Gel and Vapour-Liquid-Solid Methods. *Nano Vis.*, **1**(1): 47–53.
10. Bragg, W.H. and Bragg, W.L. **1918**. *X Rays and Crystal Structure*. London: G. Bell and Sons, LTD.
11. P. Scherrer, P. **1918**. Bestimmung der Größe und der inneren Struktur von Kolloidteilchen mittels Röntgenstrahlen." *Nachrichten von der Gesellschaft der Wissenschaften zu Göttingen, Mathematisch-Physikalische Klasse* *Göttinger Nachrichten Gesell.*, **2**: 98-100.